# Ground Current Prediction Methodology Employing RIME-CNN-LSTM-Attention Architecture


**Abstract**

The secure and dependable functioning of high-voltage cable networks relies on the accurate prediction of ground currents. This research introduces a groundbreaking prediction framework, termed RIME-CNN-LSTM-Attention, which leverages the Rime optimization algorithm to enhance the architecture of Long Short-Term Memory networks (LSTM). The framework integrates Convolutional Neural Networks (CNN) and attention mechanisms to establish a robust predictive backbone. The adaptability of the RIME algorithm is instrumental in optimizing critical hyperparameters such as learning rate, hidden layer dimensions, and regularization coefficients, thereby enhancing the model's global optimization capabilities and reducing the likelihood of converging to suboptimal local optima. The main goal of this research is to create a prediction model for ground currents with a high degree of accuracy, which is crucial for ensuring the secure monitoring and upkeep of high-voltage cable networks. Empirical results validate the exceptional performance of the RIME-CNN-LSTM-Attention model, demonstrating significant reductions in Root Mean Square Error (RMSE) by 57.12%, 51.90%, and 39.95% compared to CNN, LSTM, and CNN-LSTM-Attention models, respectively. This novel approach not only provides robust technical support for the management and maintenance of high-voltage cable systems but also paves new pathways for time-series forecasting research. The study underscores the model's superior predictive performance and robustness, highlighting its substantial academic and engineering significance.



**Keywords**: Ground current prediction; Long short-term memory networks; Rime optimization algorithm; Time-series forecasting; Hyperparameter optimization.


## 1. Introduction

As China's urbanization accelerates, the dependable operation of urban power systems—critical infrastructure for city development—has become increasingly vital. This is especially pronounced in teeming metropolises with high population densities and robust economic activity, where the demand for electricity is rising, and the performance standards for power transmission media, particularly high-voltage cables, are becoming ever more exacting [1-3]. High-voltage cables, as the main channels for power transmission, are subjected to extended periods of high-load operation that severely test the resilience of cable insulation materials [4], significantly heightening the risk of cable failures. Among the various indicators of faults, variations in the grounding current of high-voltage cables have emerged as a crucial diagnostic indicator of the condition of cable insulation. The occurrence of grounding current often signals insulation issues within the cable, damage to the metallic sheath, or flaws in the grounding system. Consequently, the ability to accurately predict changes in the grounding current of high-voltage cables is essential for the timely detection of cable faults and the prevention of power system outages [5].

However, the predictive accuracy and broad applicability of conventional physical models and empirical formulas in forecasting high-voltage cable grounding currents are significantly constrained due to the challenge of accounting for the intricate grid environment and the variable operational conditions. In recent years, the rapid advancement of deep learning technology has introduced novel approaches to high-voltage cable grounding current prediction. Deep learning models can autonomously extract complex features from data and generate precise predictions based on these features, offering robust support for the stable operation of power systems [6]. Hence, this paper proposes a RIME-CNN-LSTM-Attention-based time series prediction model tailored for forecasting grounding currents in high-voltage cables. The model is designed to address the limitations of traditional methods, enhance prediction accuracy and robustness, and provide reliable technical support for the preventive maintenance and fault warning of power systems. By employing this model, we aim to achieve accurate prediction of high-voltage cable grounding currents, thereby ensuring the secure and uninterrupted operation of the power system.

Within the power system domain, there have been research efforts to apply deep learning techniques to the prediction of high-voltage cable grounding current [7]. Studies [8-15] primarily focus on short circuit current prediction methods, including the use of distribution models, wavelet transform, least squares, neural networks, and others, with the goal of improving prediction accuracy and efficiency. Nevertheless, these methods face limitations when applied to the prediction of grounding current in high-voltage cables, such as issues with model complexity and data processing capability. In the realm of deep neural networks, scholarly works [16-21] have proposed groundbreaking methods for forecasting the grounding current in high-voltage cables. These academic endeavors utilize various deep learning architectures, including convolutional neural networks (CNN), long short-term memory networks (LSTM), and extreme learning machines (ELM), to construct accurate and effective predictive frameworks that merge temporal data series with extrinsic impact variables. Among them, literature [16] achieved accurate power load prediction by transforming time series data into images for processing and clustering using a CNN model. Literature [17] proposed a scalable prediction model through the combination of CNN and K-means clustering algorithm. Literature [18] introduced the deep learning model, which delivered highly accurate results in load forecasting. Conversely, literature [19] investigated load forecasting based on deep residual networks. Literature [20] and [21] applied deep learning models such as CNN and support vector machines (SVM) to cable short-circuit and grounded capacitor current prediction, respectively, showcasing the potential for widespread application of deep learning in the field of power system prediction.

In view of the above challenges and the increasing capability of deep learning, this study comprehensively explores methods to improve the predictability of ground currents in high voltage cables. The research objective is to design a RIME-CNN-LSTM-Attention model that utilizes the advantages of deep learning algorithms to overcome the limitations of traditional prediction methods. By integrating the advanced feature extraction capability of CNN, the sequence modeling proficiency of LSTM, and the attention of the attention mechanism to relevant data points, the proposed model aims to achieve higher prediction accuracy and robustness. The Rime optimization algorithm is applied to further optimize the hyperparameters of the model to ensure the best performance. The empirical results presented in this paper confirm the validity of the proposed model, demonstrating its ability to predict ground currents with high accuracy, thus facilitating timely fault detection and outage prevention. The significance of this research extends beyond its direct application to high-voltage cable systems; it paves new pathways for the application of deep learning in the broader domain of power system prediction and maintenance, thereby supporting the sustainable and resilient operation of urban electrical infrastructures.

## 2. Related work

### 2.1The Rime Optimization Algorithm

Hang Su [22] introduced the Rime Optimization Algorithm (RIME) in February of 2023, which proves to be a successful optimization technique leveraging the natural occurrence of rime ice. This algorithm, known as RIME, integrates the dual strategies of exploration and exploitation within its optimization approach through mimicking the expansion processes of both soft and hard rime types. The algorithm devises a strategy for navigating soft rime and a piercing approach for hard rime, facilitating an adaptable transition between extensive exploration and focused exploitation to identify the best possible solution. Hard-rime growth can efficiently converge towards the global near-optimal solution by intersecting the present solution with the optimal solution, enhancing accuracy and efficiency. RIME filters away inferior answers and deliberately offers less than optimal options to improve the greedy selection process. This enhances population diversity and avoids the algorithm from being trapped in local optima. The approach is versatile and can be used to a wide variety of intricate optimization tasks. Each particle's condensation process is succinctly recreated, as depicted in Figure 1.

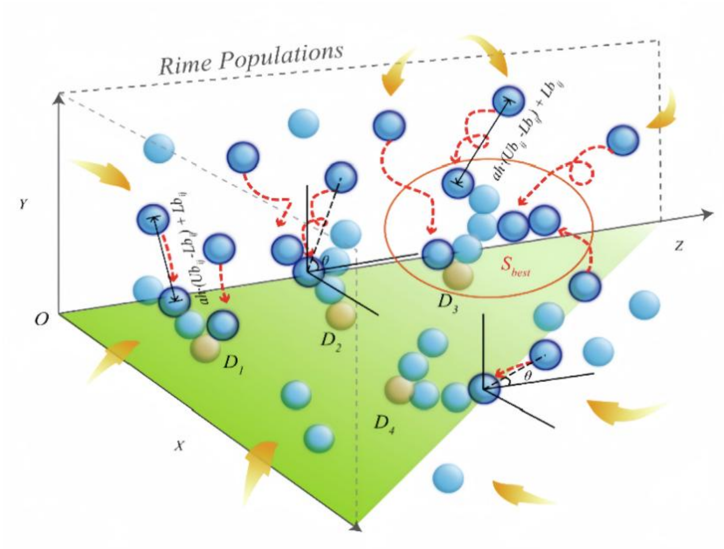


Figure 1 Soft-rime particles motion [22]

The position of the frost particles is shown in equation (1)

$$R_{ij}^{\mathrm{new}} = R_{best,j} + r_1 \cdot cos\,\theta \cdot \beta \cdot (h \cdot (Ub_{ij} - Lb_{ij}) + Lb_{ij}), r_2 < E \tag{1}$$

Where,

$$\theta = \pi \cdot \frac{t}{10 \cdot T} \tag{2}$$

$$\beta = 1 - \left[\frac{w \cdot t}{T}\right] / w \tag{3}$$

$$E = \sqrt{(t/T)} \tag{4}$$

$R_{\mathrm{ij}}^{\mathrm{new}}$ X represents the updated location of a particle, where i and j indicate the j-th particle within the i-th rime-agent cluster; $R_{\mathrm{best,j}}$ signifies the j-th particle of the top-performing rime-agent within the rime-population, R; $\beta$ denotes the environmental factor, which varies with the number of iterations to mimic the impact of the external surroundings and is crucial for guaranteeing the convergence of the algorithm. E represents the attachment coefficient, influencing the likelihood of an agent's condensation and rising as the iteration count progresses, as depicted in equation (4).

Figure 2 illustrates the puncture phenomenon.

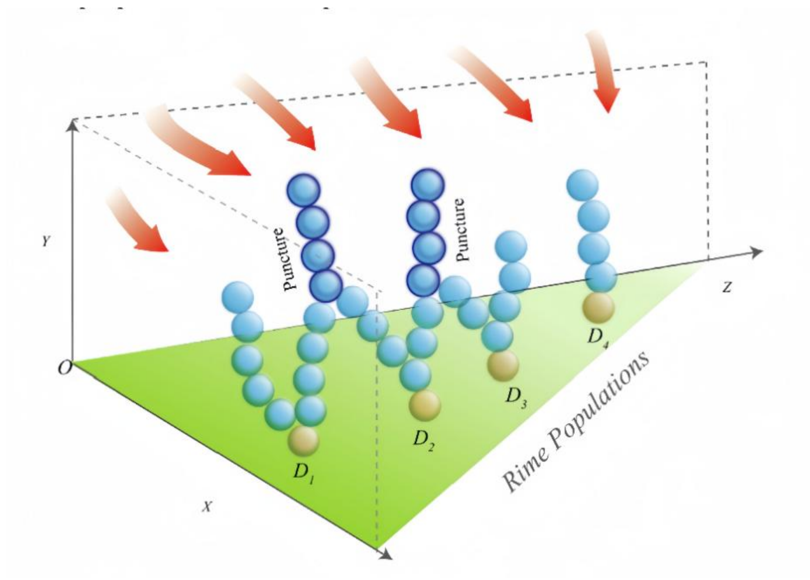


Figure 2 Hard-rime puncturing [22]

Equation (5) displays the formula used for the particle replacement process.

$$R_{ij}^{new} = R_{best,j}, r_3 < F^{normr}(S_i) \qquad (5)$$

Where， $F^{normr}(S_i)$ represents the normalized fitness value of the current agent, which signifies the probability of the i-th rime-agent being chosen.

**2.2Long Short-Term Memory**

Long Short-Term Memory (LSTM) networks are a type of advanced neural network architecture specifically designed to overcome the long-term dependency problem inherent in traditional Recurrent Neural Networks (RNNs). Thanks to its unique structure, the LSTM is adept at capturing and processing long-term dependencies within time-series datasets. Central to the LSTM's functionality is the memory cell, as described in reference [23] and visualized in Figure 3.

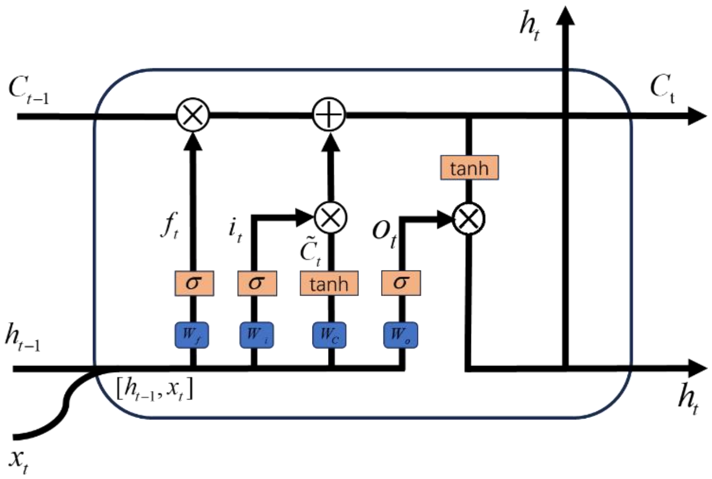


Figure 3 Structure of LSTM network

The memory unit regulates the transfer and updating of information through three gating structures, following the equations [24].

$$C_t = f_t \circ C_{t-1} + i_t \circ \widetilde{C}_t \qquad (6)$$

$$f_t = \sigma(W_f \cdot [h_{t-1}, x_t] + b_f)$$
(7)

$$i_t = \sigma(W_i \cdot [h_{t-1}, x_t] + b_i)$$
(8)

$$\widetilde{C}_t = tanh\,(W_C \cdot [h_{t-1}, x_t] + b_C)$$
(9)

$$o_t = \sigma(W_o \cdot [h_{t-1}, x_t] + b_o)$$
(10)

$$h_t = o_t \circ tanh\,(C_t)$$
(11)

In the LSTM network, the vector $[h_{t-1}, x]$ is formed by concatenating the hidden state from the previous time step, $h_{t-1}$, with the current input, x. The variable $W_f$ denotes the weights associated with the forgetting gate, while $b_f$ is the corresponding bias term. $W_c$ and $b_c$ are the weights and bias for the memory cell, respectively. $W_i$ and $b_i$ are the weights and bias for the input gate, and $W_o$ along with $b_o$ are the weights and bias for the output gate, respectively.

The LSTM network is capable of dynamically and selectively forgetting, modifying, and emitting information, which suits it particularly well for capturing long-term dependencies. These networks are particularly adept at handling time-series data, especially in scenarios that involve the need to track long-range dependencies.

**2.3Attention Mechanism**

The Attention Mechanism (AM) replicates human attention by directing the model to certain sections of information processing, enhancing the model's ability to concentrate on crucial information and hence enhancing its effectiveness in handling the input. Bahdanau et al. (2014) and Luong et al. (2015), cited in reference [25], are recognized for their seminal contributions to the development of Attention Mechanisms within deep learning. Their research introduces an attention mechanism that assigns weights to the features extracted by the preceding layers C and LSTM, enabling the model to focus on the spatiotemporal aspects of the original sequence. These weighted features are then fed into the model to generate predictions. Figure 4 provides a visual representation of the attention mechanism's architecture. By employing this approach, the expectation model can gain a deeper insight into the inherent structure of the input data, thereby enhancing the precision of its predictive outcomes.

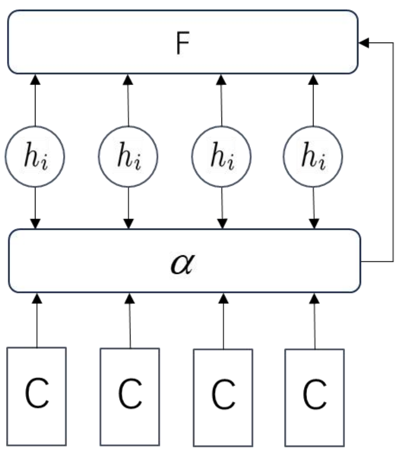


Figure 4 Attention structure diagram

$$\varphi(h_i, C) = tanh\,(h_i \cdot W_\alpha \cdot C_t + b_\alpha)$$
(12)

$$\alpha_i = \frac{exp\,(\varphi(h_i, C))}{\sum_{j=1}^{n} exp\,(\varphi(h_j, C))}$$
（13）

$$F = \sum_{i=1}^{n} \alpha_i \, h_i \qquad (14)$$

In the above equations [14], C denotes the feature vector obtained after processing through the CNN network, while hi represents the feature vector extracted by the LSTM network at the i-th time step. x corresponds to the weight, and y represents the bias term. Equation (12) is designed to weigh the features extracted from both the CNN and LSTM networks, and it achieves the fusion of these weights through an activation function. Equation (13) is to pass the weights through softmax function. Ultimately, the final set of features is derived by multiplying the LSTM's output values with the corresponding weights, as specified in equation (14). These weighted features are subsequently fed into a series of fully connected layers, which then produce the final predicted outcomes.

## 3. Methods RIME-CNN-LSTM-Attention Model

In the LSTM neural network model, the parameter configuration exerts a critical influence on the model's recognition accuracy. Conventionally, hyperparameter selection tends to rely on empirical methods, which are characterized by a degree of arbitrariness and lack of systematic guidance. This approach often results in instability and a lack of generalizability in the model's performance. To tackle this challenge, the present study utilizes the Frost Optimization Algorithm (RIME) to identify optimal settings for three critical hyperparameters of the LSTM model: the initial learning rate, the number of neurons in the hidden layer, and the most suitable L2 regularization coefficient.

The learning rate governs the magnitude of weight updates during training. Typically, it is set within the range of 0.001 to 0.1. A learning rate that is too low might lead to overfitting, as the model may become too finely tuned to the training data. Conversely, a learning rate that is too high can cause the loss function to oscillate wildly, preventing the model from converging effectively. The number of nodes in the hidden layer is a key factor that influences the model's complexity and its ability to capture and represent the underlying patterns in the data. Insufficient nodes may fail to meet the training requirements, while an excessive number can lead to an overly complex model structure, prolonging training time. The regularization parameter serves to reduce the complexity of the LSTM model, enhancing its generalization capability and mitigating the risk of overfitting. Figure 5 depicts the flowchart of the optimization process.

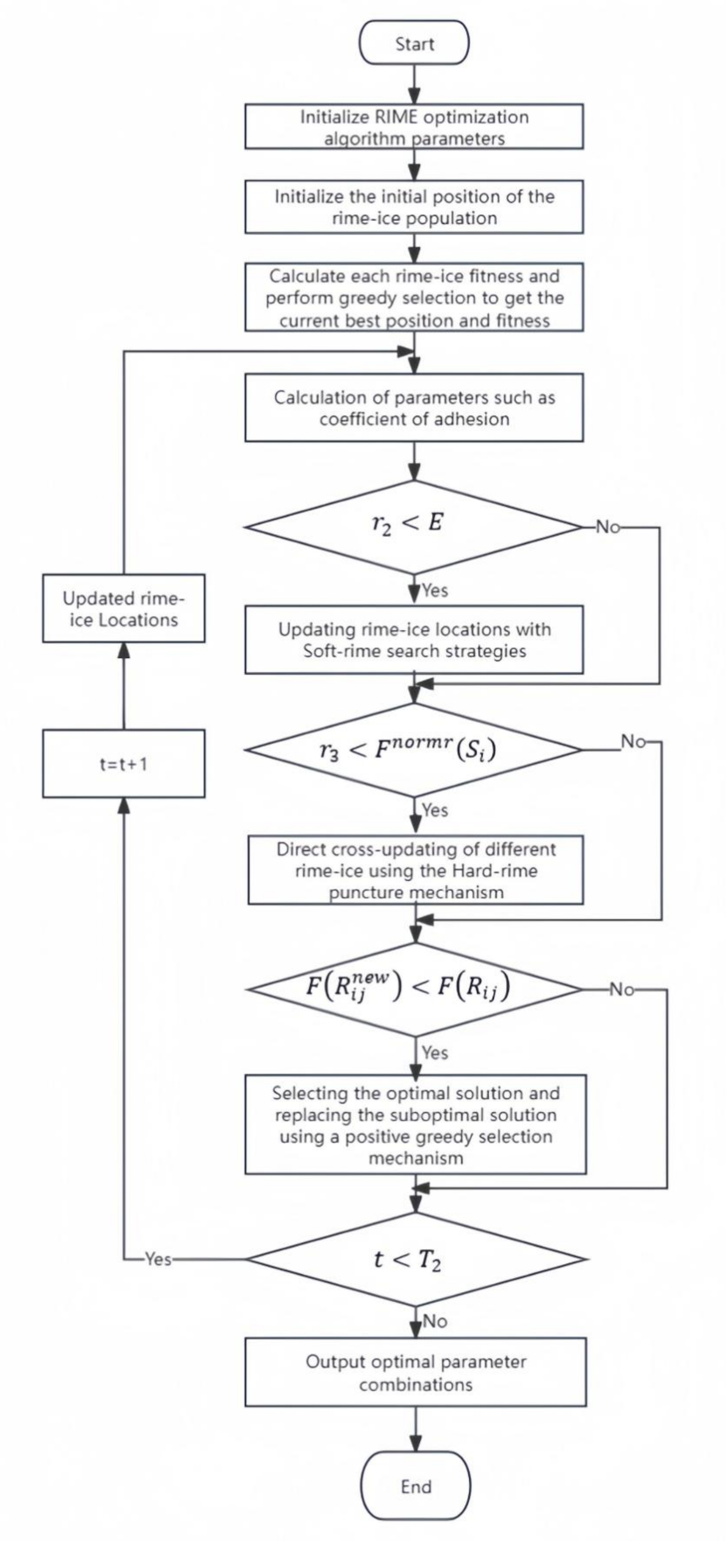


Figure 5 Flowchart of RIME optimized LSTM parameters

The objective of this optimization routine is to pinpoint the parameter configurations for the LSTM model that most effectively align with the dataset, thereby enhancing the model's classification accuracy and its efficacy when dealing with extensive data samples. The architecture of the RIME-CNN-LSTM-Attention model proposed in this research is outlined in Figure 6 below.

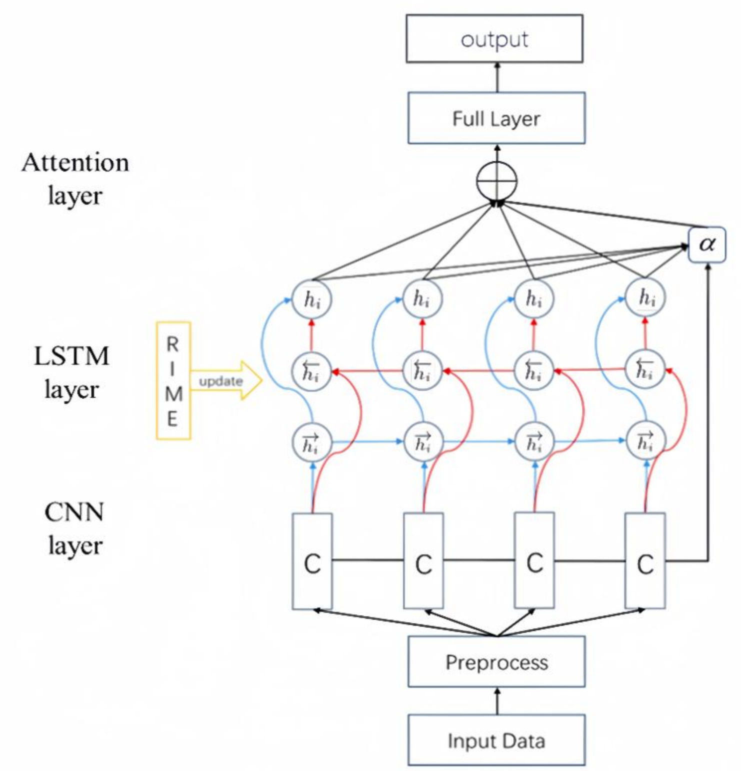


Figure 6 Structure of the RIME-CNN-LSTM-Attention model

The workflow of the RIME-CNN-LSTM-Attention ground current prediction algorithm, which incorporates the RIME-CNN-Attention framework designed in this paper, is delineated as follows:

Step 1: Preprocess the actual ground current data from the monitoring point to serve as input for the model.

Step 2: Employ CNN to perform convolutional computations and extract the foundational features from the multi-dimensional data.

Step 3: The RIME optimization algorithm is applied to fine-tune the hyperparameters of the LSTM network, after which the optimized LSTM is used to extract sequential features.

Step 4: Employ the Attention mechanism to apply weightings to and fuse the extracted features, thereby enhancing their significance and representation.

Step 5: Transmit the processed features through a fully connected layer to consolidate the information.

Step 6: Derive the ground current prediction and conclude the process.

This sequence ensures a systematic and comprehensive approach to ground current prediction, leveraging the strengths of each component in the hybrid model to achieve accurate and reliable forecasts.

## 4. Experimental procedures and data analysis

### 4.1Experimental data

The dataset for this experiment is comprised of actual grounding current data from a cable line in Beijing, spanning from January 1, 2018, to December 30, 2018. The data were sampled daily, encompassing a total of 50 monitoring points for ground current. Given the susceptibility of the measured data to various environmental factors and the presence of missing values within the dataset, a preprocessing step was undertaken to address these issues. To handle missing data [26], two strategies were implemented: monitoring points with more than 50% missing data were excluded from the dataset, whereas those with 50% or less missing data were interpolated using the median value. Following this data cleansing process, a dataset of ground current from 47 monitoring points was compiled, which forms the foundation for subsequent experimental analysis.

To provide a clearer visualization of the ground current distribution at the monitoring points, a random monitoring point was chosen for graphical representation, as shown in Figure 7 below.

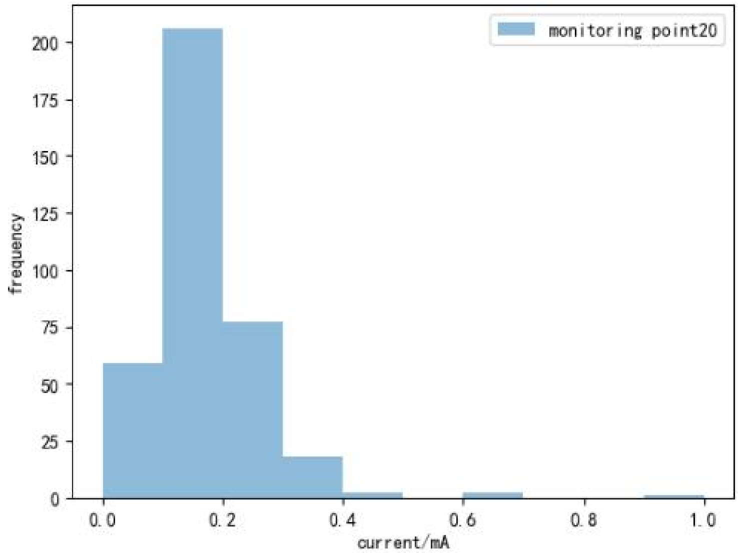


Figure 7 Ground current distribution at monitoring point 20

Figure 7 illustrates that the ground currents recorded at monitoring point 20 predominantly fall within the range of 0 to 0.4 mA, suggesting that the ground currents are generally low for the majority of the time. Nonetheless, there are instances where the ground current exceeds 0.6 mA, which could be attributed to certain specific events or abnormal conditions.

To provide a comprehensive view of the distribution of ground currents across all monitoring points, Figure 8 is presented below. This figure will further elucidate the variability and patterns of ground currents within the entire dataset.

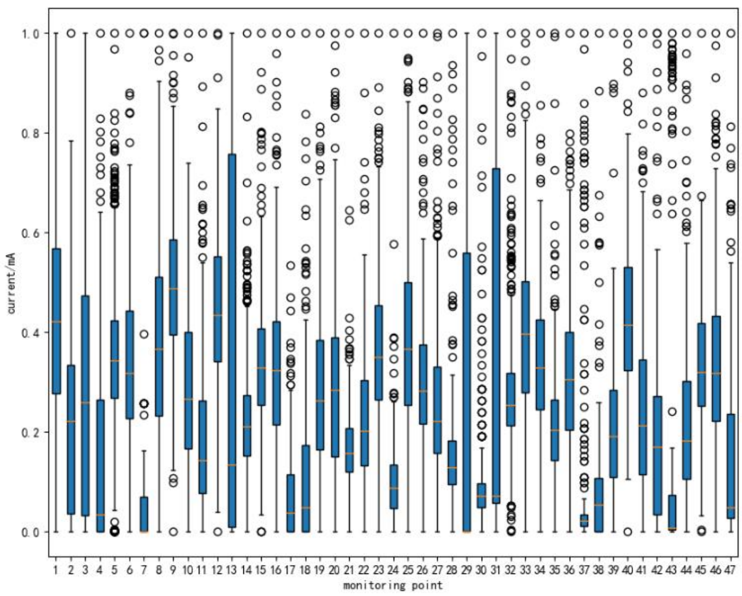


Figure 8 Ground current box diagram for all monitoring points

The descriptive statistics, complemented by the visualization of box plots, reveal that the mean values of ground currents across all monitoring points lie within the range of 0.288 to 0.328, while the standard deviations fall between 0.184 and 0.215, signifying a moderate level of data dispersion. The majority of minimum values are at 0, although some monitoring points exhibit slightly higher minimums, which could be attributed to measurement inaccuracies or artifacts of the data preprocessing stage. The median values are slightly greater than the means, suggesting a potential right-skew in the data distribution. The box height and whisker length in the box plots provide insights into the variability of ground current data at different sites. Sites with taller boxes and longer whiskers indicate greater variability in ground currents, which may be influenced by specific environmental factors or occurrences. Additionally, a few monitoring points exhibit outliers that significantly deviate from the rest of the data, potentially indicating unique events or anomalies, such as equipment malfunctions, severe weather conditions, or human interventions.

**4.2Evaluation Criteria**

The Root Mean Squared Error (RMSE) and Mean Absolute Error (MAE) were chosen as the evaluation metrics for the model, as referenced in [27], and are defined by the following equations.

$$\mathrm{MAE} = \frac{1}{N}\sum_{N}^{m=1}\left|\widehat{Z}(m) - Z(m)\right| \quad (15)$$

$$\mathrm{RMSE} = \sqrt{\frac{1}{N}\sum_{N}^{m=1}\left(Z(m) - \widehat{Z}(m)\right)^2} \quad (16)$$

**4.3RIME parameter optimization**

The dataset is partitioned such that 70% of the data is assigned to the training set, which is used for model training, and the remaining 30% is set aside as the test set, used to assess the model's efficacy.

The preliminary parameter settings for the optimized model are outlined in Table 1. The parameters subject to optimization are the number of units in the hidden layer, the starting learning rate, and the optimal L2 regularization coefficient.

Table 1 Initial Parameter Values of the Optimization Model.

| Parameters | Value(or range of values) |
|---|---|
| Population size | 6 |
| Maximum number of iterations | 10 |
| Number of optimization parameters | 3 |
| Number of hidden layer units | [4,128] |
| Initial learning rate | 0.1,0.01,0.001 |
| Optimal L2 regularization factor | [0.00001,0.01] |

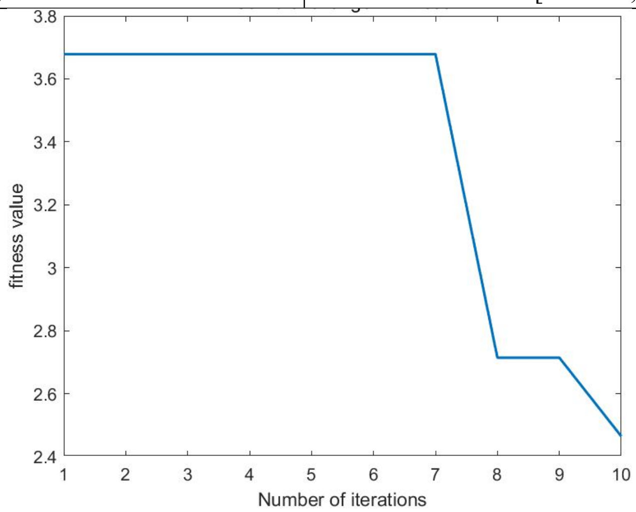


Figure 9 Optimization algorithm fitness change curve

As the iteration progresses, the RIME algorithm continuously refines and updates the number of hidden layer units, the initial learning rate, and the optimal L2 regularization coefficient. The convergence curve is depicted in Figure 9, revealing the optimal hyperparameters: the optimal number of hidden layer units is 96, the optimal initial learning rate is 0.01, and the optimal L2 regularization coefficient is 0.00017.

**4.4Analysis of experimental results**

With the optimized parameters established by the RIME algorithm, the architecture of the RIME-CNN-LSTM-Attention network is accordingly defined. Figures 10 and 11 provide comparative graphs showing the actual versus predicted ground currents for every monitoring point in the training set and the test set, respectively. These visual comparisons enable a straightforward evaluation of the model's accuracy during both the training and testing stages. Figure 12 and Figure 13, on the other hand, display the error curves for the ground current predictions at each monitoring point in the training and test sets, providing insights into the accuracy and consistency of the model's predictions.

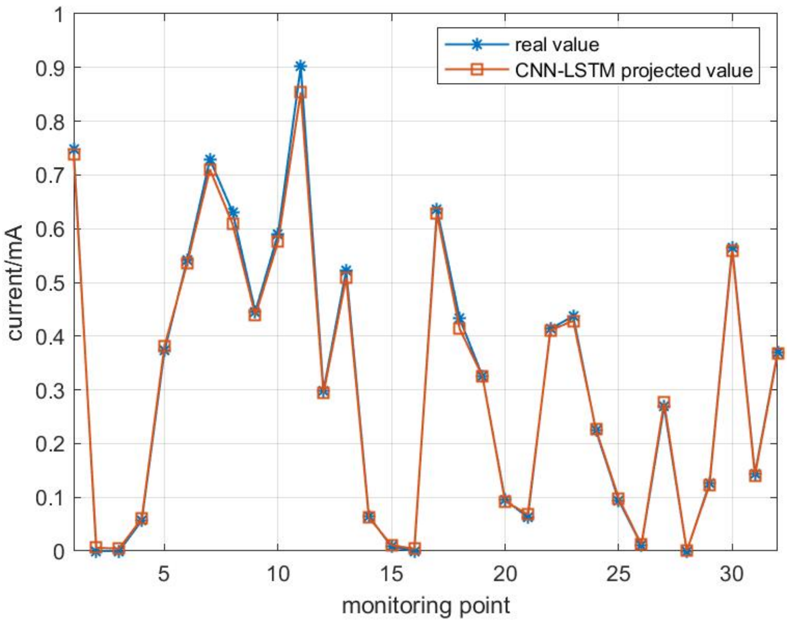


Figure 10 Comparison of training set predictions

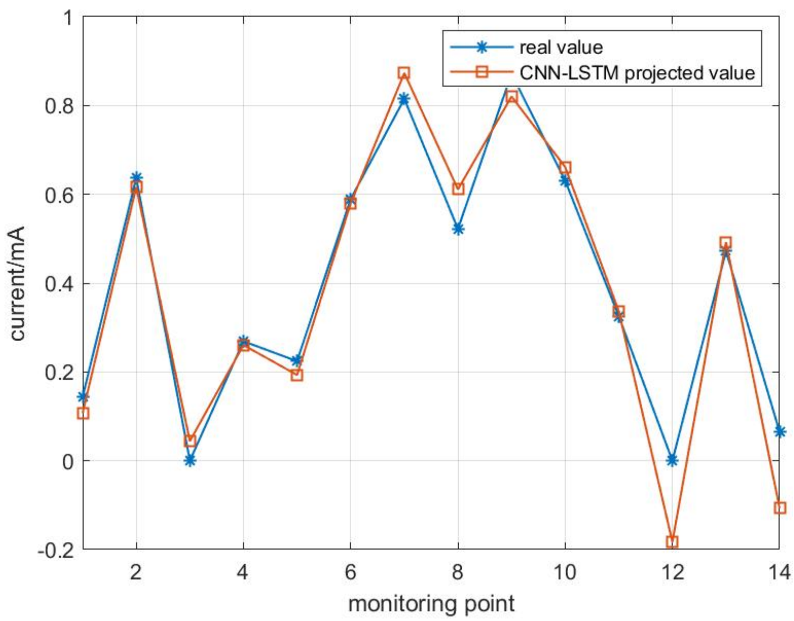


Figure 11 Comparison of test set predictions

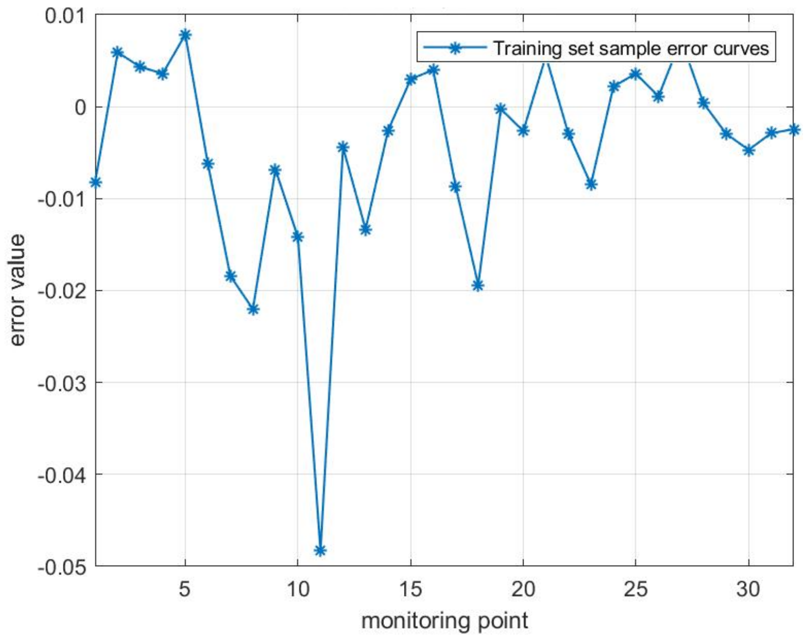


Figure 12 Sample error curves for the training set

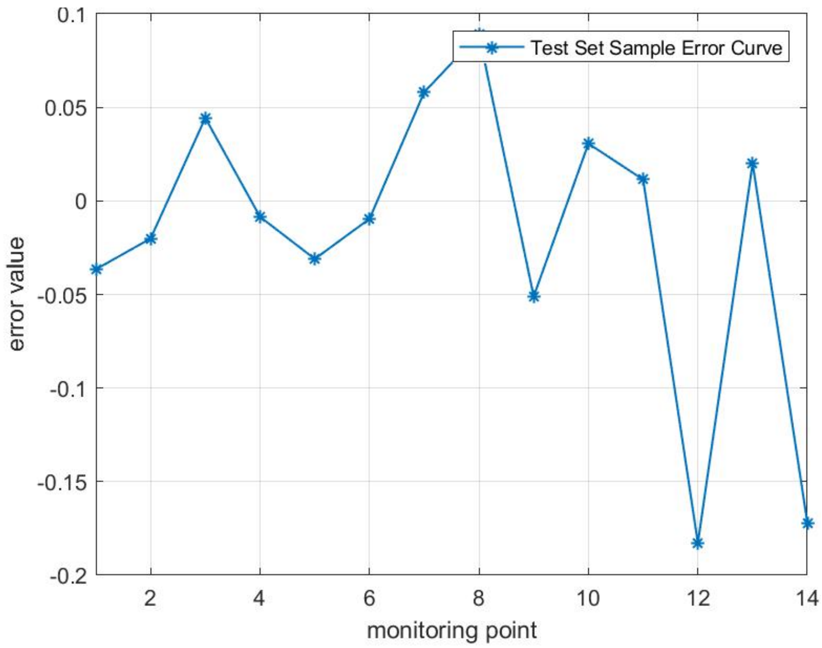


Figure 13 Sample error curve for the test set

Table 2 Model performance evaluation table

| | RMSE | MAE | $R^2$ |
|---|---|---|---|
| Training set | 0.0119 | 0.0078 | 0.9979 |
| Test set | 0.0771 | 0.0547 | 0.9251 |

The statistics outlined in Table 2 highlight the model's outstanding performance on the training dataset, with an $R^2$ value close to 1, and remarkably low RMSE and MAE values. These indicators suggest an almost ideal alignment with the training data. Nevertheless, when the model is assessed on the test dataset, there is a noticeable drop in its performance, which points to the likelihood of overfitting. Overfitting happens when a model is excessively intricate or has memorized the training data, including its noise, leading to suboptimal performance on previously unencountered data.

The $R^2$ value of 0.9251 for the test set, while considerable, is substantially lower than that for the training set, signifying a reduced ability of the model to predict accurately on novel data. This discrepancy suggests that the model may be capturing idiosyncrasies in the training data that do not translate well to the test set, leading to a loss of predictive precision for new observations.

Table 3 Evaluating the predictive outcomes across various model types

| Models | RMSE |
|---|---|
| CNN | 0.1798 |
| LSTM | 0.1603 |
| CNN-LSTM-Attention | 0.1284 |
| RIME-CNN-LSTM-Attention | 0.0771 |

Table 3 offers a comparative analysis of the experimental outcomes for various deep learning models applied to the ground current prediction task using the dataset under consideration. Notably, the results demonstrate a significant disparity among the models. Each model outperforms the traditional CNN, suggesting that the integration of temporal feature extraction and the attention mechanism significantly enhances the model's predictive capabilities.

Furthermore, the hybrid model, which combines CNN, LSTM, and Attention, outperforms the individual components. This suggests that when dealing with large-scale data, a single model may struggle to fully capture the intricate interrelationships within the data. The hybrid model's approach, however, bolsters the model's capacity to extract and represent data features effectively.

The inclusion of bi-directional LSTM encoding in the model facilitates a more comprehensive capture of features across different contexts, contributing to improved performance. Additionally, the use of Attention ensures that the model assigns appropriate weights to the features, leading to more robust detection results.

The CNN-LSTM-Attention model, after optimization, achieves a significantly reduced RMSE of 0.1284. Subsequent optimization of the model using the RIME algorithm further enhances its overall performance, with the RMSE being reduced to 0.0771. This outcome corroborates the efficacy of the proposed model as outlined in this paper.

## 5. Discussion

This research presents an innovative deep learning architecture, the RIME-CNN-LSTM-Attention model, designed to tackle the complex task of forecasting ground currents in high-voltage cable systems. The research yielded the following key findings:

(1) Model Innovation: The combination of CNN, LSTM, and the Attention mechanism works in concert to effectively encapsulate spatial, temporal, and pivotal information from the data, significantly improving the model's predictive precision and resilience.

(2) Hyperparameter Optimization: The application of the RIME algorithm for optimizing the LSTM network's hyperparameters prevents the model from converging to local optima and improves its generalization capabilities and prediction accuracy.

(3) Performance Enhancement: The proposed RIME-CNN-LSTM-Attention model exhibits substantial enhancements in performance metrics like RMSE (Root Mean Square Error) and MAE (Mean Absolute Error) when contrasted with conventional CNN, LSTM, and CNN-LSTM-Attention models, highlighting its effectiveness and advantage.

## Refrences


[1] Wu Ming. Design and research of online monitoring system for ground loop current of XLPE cable based on GPRS [D]. Wuhan University of Technology,2014.

[2] Dong Huanyu. Research on online monitoring system of ground loop current of high voltage cable[D]. Shenyang Engineering Institute,2017.

[3] YANG Jingbo,WU Xinqiang,YU Jianyou,et al. Research on the design of online monitoring of cable ground loop current[J]. Communication Power Technology,2017,34(01):107-108.
[4] LU Chaofeng,SHEN Jiahua,ZHANG Jialin,et al. Design and research of online monitoring system for grounding current of high voltage cable[J]. Electrotechnology,2024,(02):26-28+93.
[5] Luo Yan. Front-end design and realization of online monitoring system for ground loop current in high voltage cables[D]. Huazhong University of Science and Technology,2021.
[6] MAO Yuanhong,SUN Chenchen,XU Luyu,et al. A review of time series forecasting methods based on deep learning[J]. Microelectronics and Computers,2023,40(04):8-17.
[7] LIANG Hongtao,LIU Shuo,DU Junwei,et al. A review of research on deep learning applied to timing prediction[J]. Computer Science and Exploration,2023,17(06):1285-1300.
[8] XU Xian.A new method and application of short-circuit current prediction for 220kV grid[J]. Power System Automation,2007,(16):103-106.
[9] CHEN Li'an, ZHANG Peiming, MU Xiren. Early prediction of short-circuit faults in low-voltage systems based on wavelet transform[J]. Journal of Electrotechnology,2003,(02):91-94.
[10] C.Y. Chen, L.A. Chen, X.R. Mu, et al. Algorithm study on early prediction of peak short-circuit current for selective protection of low-voltage distribution system[J]. Journal of Fuzhou University(Natural Science Edition),2015,43(03):359-364.
[11] ZHANG Yitao,WANG Zezhong,LIU Liping,et al. Line loss prediction of 10 kV distribution network based on gray correlation analysis and improved neural network[J]. Grid Technology,2019,43(04):1404-1410.
[12] Li-an C. Prediction for magnitude of short circuit current in power distribution system based on ANN[C]//2011 International Symposium on Computer Science and Society. IEEE, 2011: 130-133.
[13] Xiren Miao,Xiaomei Wu. Early detection and prediction of multilevel short-circuit current in low voltage systems[J]. Journal of Electrotechnology,2014,29(11):177-183.
[14] CHEN Jianming,ZHANG Panpan. Application of gray BP neural network model in peak short-circuit current prediction of power syste
[15] WANG Mengjiao,WEI Xinlao. Particle swarm optimization limit learning machine for short-circuit current prediction technique[J]. Journal of Electrical Machines and Control,2022,26(01):68-76.m[J]. Journal of Light Industry,2018,33(04):79-85.
[16] Li L, Ota K, Dong M. Everything is image: CNN-based short-term electrical load forecasting for smart grid[C]//2017 14th international symposium on pervasive systems, algorithms and networks & 2017 11th international conference on frontier of computer science and technology & 2017 third international symposium of creative computing (ISPAN-FCST-ISCC). IEEE, 2017: 344-351.
[17] Dong X, Qian L, Huang L. Short-term load forecasting in smart grid: a combined CNN and K-means clustering approach[C]//2017 IEEE international conference on big data and smart computing (BigComp). IEEE, 2017: 119-125.
[18] Kuo P H, Huang C J. A high precision artificial neural networks model for short-term energy load forecasting[J]. Energies, 2018, 11(1): 213.
[19] Chen K, Chen K, Wang Q, et al. Short-term load forecasting with deep residual networks[J]. IEEE Transactions on Smart Grid, 2018, 10(4): 3943-3952.
[20] Lianbing Li, Liangliang Dai, Jingpeng Li, et al. Research on short-circuit current prediction for cables based on improved VMD-CNN[J/OL]. China Test,1-11[2024-06-05].
[21] WANG Qingliang,LI Shuchao,CHEN Xuan,et al. Prediction method of single-phase grounded capacitive current in coal mine power grid based on model migration and SVM[J]. Journal of Xi'an University of Science and Technology,2024,44(01):155-165.
[22] Hang S ,Dong Z ,Asghar A H , et al. RIME: A physics-based optimization[J].Neurocomputing,2023,532183-214.
[23] Sherkatghanad Z ,Ghazanfari A ,Makarenkov V .A self-attention-based CNN-Bi-LSTM model for accurate state-of-charge estimation of lithium-ion batteries[J].Journal of Energy Storage,2024,88111524-.
[24] Song X ,Wang Z ,Wang H .Short-term load prediction with LSTM and FCNN models Based on attention mechanisms[J].Journal of Physics: Conference Series Journal of Physics: Conference Series ,2024,2741(1).
[25] Xiao Y .An Overview of the Attention Mechanisms in Computer Vision[J].Journal of Physics: Conference Series,2020,1693(1):012173-.
[26] Jia Q ,Dongsheng Y ,Bowen Z , et al. Semi-supervised variational bi-directional sampling on multi-class imbalanced electric power data for fault diagnosis[J].International Journal of Electrical Power and Energy Systems,2024,155(PA).
[27] Z. Ouyang, J. Sun, X. Zhao, Y. Shen and S. Li, "Short-term wind power prediction model based on PCA-GA-LSTM neural network," 2023 IEEE 6th International Electrical and Energy Conference (CIEEC), Hefei, China, 2023, pp. 148-153, doi: 10.1109/CIEEC58067.2023.10166020.